PNAS RESEARCH ARTICLE | EARTH, ATMOSPHERIC, AND PLANETARY SCIENCES OPEN ACCESS

Proximal ejecta of the Bolaven extraterrestrial impact, southern Laos

Kerry Sieh[a,b,c,d,1], Dayana Schonwalder Angel[a,e], Jason Herrin[a,f], Brian Jicha[g], Brad Singer[g], Vanpheng Sihavong[h], Weerachat Wiwegwin[i], Nathanael Wong[a,b,j], and Jia Yong Quah[a,b,k]

Contributed by Kerry Sieh; received June 19, 2023; accepted October 24, 2023; reviewed by Ryuji Tada and Paul A. Carling

Sediments in southern Laos and eastern Thailand confirm that the Australasian tektite strewn field came from an extraterrestrial impact crater on the Bolaven Plateau of southern Laos. The principal evidence is the Bolaven diamicton, a pebbly to bouldery breccia that is thickest and coarsest on the plateau. Tektites, the melted target material strewn widely by the forces of the impact 789.0 ± 1.8 ka ago, lie either within the uppermost part of the diamicton or atop it. On the flanks of the plateau, the basal diamicton often contains clasts from preimpact lavas and gravels and sometimes mantles broken Mesozoic bedrock. Locally, its upper portions contain unweathered boulders of basalt or sandstone. Its sharp upper contact with a thick sandy silt implies that the two beds formed in rapid succession. These characteristics of the Bolaven diamicton show that it resulted primarily from the excavation, comminution, and launch of sandstone and weathered basaltic lavas from a crater on the Bolaven Plateau, and entrained other materials while in transit.

Australasian | ejecta | impact | Laos | tektite

Australasian tektites are black, glassy, microscopic to small boulder-sized clasts found throughout much of Southeast Asia and beyond. Recent ^{40}Ar-^{39}Ar geochronology has yielded a well-constrained 788 ka date for the extraterrestrial impact that formed them (1). Unlike the tektites, other ejecta mobilized by the impact have not garnered much attention. In part this is because the impact site has been known only vaguely, by virtue of geographical patterns of tektite size and composition, to be somewhere in northern Southeast Asia. Thus, searches for proximal deposits of the ejecta blanket have lacked geographic focus. Also, mid-20th century violence in Cambodia, Laos, and Vietnam, and resultant political instabilities and unexploded ordnance hampered field work for decades thereafter.

Nonetheless, many previous studies have noted an enigmatic gravel deposit just below the tektites. Izokh and An (2, 3) reported that the tektites in Vietnam lie between a loess-like layer and a pebbly layer that, in most cases, is lateritic. Wasson et al. (4) stated that the tektites "are generally associated with a thick, ubiquitous layer of laterite" but did not describe it in enough detail to assess either its nature or origin. Fiske et al. (5) also observed that the tektites lie atop a layer of lateritic, lithic, and quartz pebbles, which they interpreted to be a nonisochronous "lag gravel" (6).

Commonly found directly above this enigmatic deposit and the tektites is a massive silty deposit, which contains microscopic tektite spherules (7). Thai geologists have called this the "catastro-loess" because they relate it to wholesale destruction of the regional landscape and biota at the time of the impact. Songtham et al. (8) suggest that it is an airfall deposit related to the impact because it is massive. Tada et al.'s (9, 10) recent detailed analyses of these beds at two sites in eastern Thailand (Huai Om, Fig. 1*B*) confirm that both beds and the tektites are undisturbed ejecta from the same impact event. They suggest that "[F]urther investigation of the lateral distribution of the ejecta deposit would provide information about the location, magnitude, and target rocks" of the impact site. That is the primary purpose of this paper.

We have proposed that the impact crater lies within the Bolaven Volcanic Field (BVF), on the Bolaven Plateau of southern Laos (Fig. 1*A*), drawing upon five independent sets of data (11). Evidence includes a basaltic component to tektite compositions, the presence of ^{40}Ar-^{39}Ar-dated basaltic lavas before the impact, postimpact ^{40}Ar-^{39}Ar ages for all lavas atop the proposed crater, a gravity anomaly of appropriate size at the site, and a nearby outcrop of probable impact ejecta consisting of shattered boulders. Nonetheless, some have not found these data compelling (9, 12). In this paper, we further test the Bolaven impact claim by examining the nature and extent of a regionally extensive bed that underlies the tektites in the region surrounding the Bolaven Plateau.

Significance

For decades, scientists have searched for the source of the most extensive spray of extraterrestrial-impact debris on Earth, the Australasian strewn field. We document a unique pebbly to bouldery breccia that points unambiguously to its source—an impact crater buried beneath lavas of the Bolaven Plateau in southern Laos. The crater's location is constrained by the breccia's thickening and coarsening onto the plateau. The stratigraphic details of this extensive and well-preserved deposit reveal important details about the processes involved in creation of the crater and its ejecta.

Author contributions: K.S., D.S.A., and J.H. designed research; K.S., D.S.A., J.H., B.J., B.S., V.S., W.W., N.W., and J.Y.Q. performed research; K.S., D.S.A., J.H., B.J., B.S., and N.W. analyzed data; and K.S. and J.H. wrote the paper.

Reviewers: R.T., Chiba Kogyo Daigaku; and P.A.C., University of Southampton.

The authors declare no competing interest.

Copyright © 2023 the Author(s). Published by PNAS. This open access article is distributed under Creative Commons Attribution-NonCommercial-NoDerivatives License 4.0 (CC BY-NC-ND).

Although PNAS asks authors to adhere to United Nations naming conventions for maps (https://www.un.org/geospatial/mapsgeo), our policy is to publish maps as provided by the authors.

[1] To whom correspondence may be addressed. Email: sieh@ntu.edu.sg.

This article contains supporting information online at https://www.pnas.org/lookup/suppl/doi:10.1073/pnas.2310351120/-/DCSupplemental.

Published December 4, 2023.

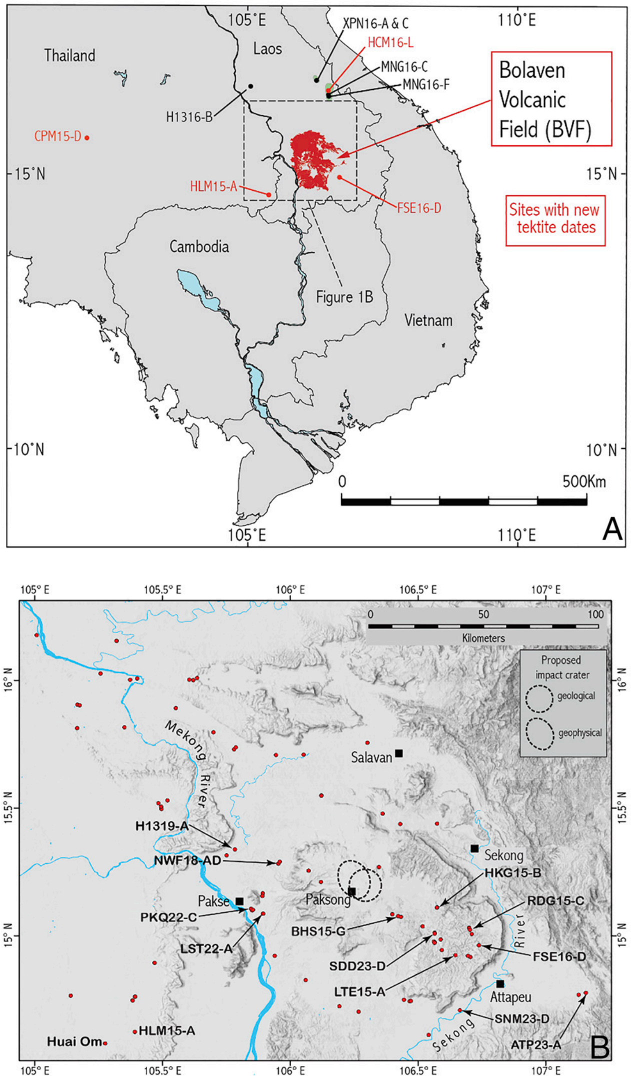

Fig. 1. Maps of distal (*A*) and proximal (*B*) sites. Labeled sites are discussed in the text. Proposed impact crater perimeters from ref. 11.

Methodology

Our field observations and collections occurred during six, weeks-long excursions from 2015 through 2023. We inspected hundreds of outcrops of BVF basalt, the tektites, and the two beds that sandwich them, mostly in roadcuts and quarry walls, nearly all within 200 km of the proposed impact site and mostly within 100 km (Fig. 1). To avoid any confusion caused by the wide range of previous descriptive terms, we refer to the enigmatic gravelly deposit hereinafter as the "diamicton," because of its wide range of clast sizes at most outcrops. We present extensive stratigraphic observations that provide two tests of its origin: First, it should thin and fine with distance from its source crater. Thus, we focus on the geographic pattern of its thickness and clast sizes, measured by tape or scale card either directly in the field or from scaled photographs. Second, its composition should be consistent with target-rock geology. If the source crater is the one that we have proposed, the diamicton's clasts and matrix should reflect the rocks of the Bolaven Plateau. We could not assess this solely by field inspection, however, so we also conducted limited geochemical analyses of the clasts and matrix to ascertain their likely protoliths. Also, to dispel from the outset any doubts that the bed is part of the Australasian strewn field, we analyzed tektites collected above and within the diamicton to see whether their composition and ages are consistent with those previously established for the Australasian impact.

Results

Thickness and constituents of the diamicton vary greatly throughout the region. Fig. 2 is a schematic summary of these complex and variable characteristics. It provides an overarching context for our detailed site-specific examinations. The stratigraphic relationship between the diamicton, tektites, and silt is everywhere the same—tektites sandwiched between the diamicton and the silt. The tektites lie either exactly at the diamicton/silt contact or within the diamicton's upper few cm. That contact is sharp, without any indication of intervening bioturbation, pedogenesis, erosion or deposition (Fig. 3). This positioning implies that all fell in rapid succession, as a result of the impact.

To ensure that the sequences we examined are indeed Australasian ejecta, we dated five tektites found in close association with the diamicton. Four of these were in situ, between the diamicton and silt bed. The ^{40}Ar-^{39}Ar dates are based on incremental heating and are detailed in *SI Appendix*, Table S1. Our date of 788.9 ± 2.4 ka is indistinguishable from a recently published 788.1 ± 2.8 ka date, an average of dates for five tektites from China, Thailand, Vietnam, and Australia (1). If one recalculates (1)'s recently determined age, using the standard age and decay constants we have used, their age becomes 789.2 ± 2.8 ka, indistinguishable from ours. An inverse-variance weighted mean of our and their data yields a very precise age of 789.0 ± 1.8 ka. More geochemical information about tektites appears in *SI Appendix* section "Geochemical Analyses …."

The diamicton commonly rests on Mesozoic bedrock (13), fluvial deposits, or Neogene basalt flows, depending on location. Rarely, that contact presents a jumble of bedrock, as in *SI Appendix*, Fig. S2 *A* and *B*. These exposures imply that some process jumbled the boulders prior to emplacement of the diamicton. In some places where the diamicton is absent or patchy, jumbled, angular sandstone blocks rest on undisturbed sandstone bedrock (*SI Appendix*, Fig. S2*C*).

Within the Diamicton.

Clasts and matrix. Two primary, nearly ubiquitous features of the diamicton are its normal grading and the predominance of highly weathered pebbles and matrix (Fig. 2). The bed is commonly framework supported and has a poorly sorted clayey to granule matrix. Gravel clasts are most commonly angular to botryoidal in shape, of very fine-grained composition, and ocherous or dark reddish brown, sometimes with a black coating. Inspection in the field suggests that many of these are broken clasts of formerly contiguous laterite, similar to that in some weathered BVF lavas (*SI Appendix*, Fig. S3*B*). Less common are angular pebbles of fine-grained sandstone. The matrix is ostensibly like the gritty saprolitic matrix of weathered BVF basalt flows on the plateau and on its flanks (*SI Appendix*, Fig. S3*A*).

We could not be certain of these BVF associations, though, simply by our field observations. Thus, we conducted geochemical analyses of matrix and clasts at several localities to determine the likely protoliths (see *SI Appendix*, Figs. S4–S6 and associated discussion). These analyses showed that High Field Strength Element (HFSE) ratios of the diamicton are in some places similar to those of Bolaven Plateau basalts and in other places similar to those of Bolaven Plateau sandstones.

Basalt boulders within the diamicton.

Site NWF18-AD. Fig. 4 shows one wall of a quarry about 35 km west-northwest of the proposed impact site. The normally graded, pebbly diamicton is capped by the silt bed. Lying ex situ on the quarry floor were many tektites, which probably fell from the diamicton/silt contact during excavation.

A solitary subrounded basalt boulder sits ~40 cm below the contact. Analysis of HFSE for the boulder and five samples of the diamicton's matrix yielded ratios that are nearly identical to each other and to unweathered basalt samples from BVF flows (Fig. 4).

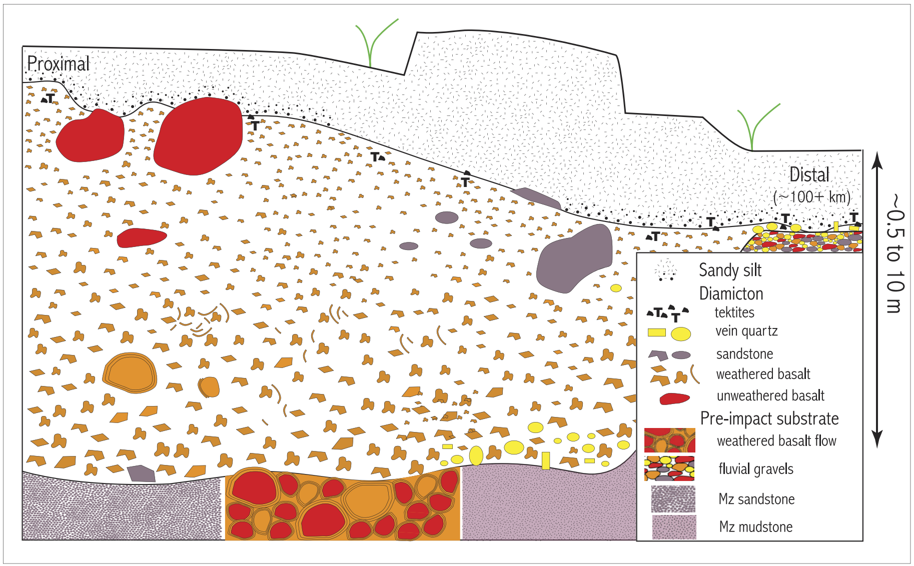

Fig. 2. Composite sketch of principal characteristics of the diamicton, from observations at many localities. No exposure contains all features.

Thus, the matrix protolith here is basaltic and likely, by virtue of its grain sizes, saprolite from a weathered flow. The silt bed's protolith also appears to be basaltic saprolite. The roundness of the boulder suggests it is a corestone from a basalt flow (as in *SI Appendix*, Fig. S3*A*). In weathered BVF basalt flows, such corestones are commonly encapsulated in hard, concentric, lateritic rinds (*SI Appendix*, Fig. S3*B*). This boulder's roundness and its lack of encapsulation implies that it acquired its shape while weathering in a preimpact lava flow and was then stripped of its lateritic rind and/or surrounding saprolite during its transit to deposition here. The ^{40}Ar-^{39}Ar age of this boulder (*SI Appendix*, Table S1) is ~1,145 ka, >300 ka older than the impact, plenty of time for a lava flow to weather to rounded corestones surrounded by saprolite before deposition within the diamicton.

Such rounded to subrounded boulders are common in the upper parts of the diamicton within about 60 km of the proposed impact crater (*SI Appendix*, Fig. S7 and Table S2). At these places, the boulders are at or very near the contact with the silt and lack concentric weathering rinds (*SI Appendix*, Figs. S8 and S9). In some instances, indentation in the diamicton-silt contact hints that the boulders fell from above and produced small craters (*SI Appendix*, Fig. S10). In other cases, what appear to have been concentrically zoned laterite rinds seem to have been stripped from their corestones and deposited independently within the diamicton (*SI Appendix*, Figs. S11 and S12). Weathered boulders of basalt occur less commonly within lower parts of the diamicton (*SI Appendix*, Fig. S12).

Sandstone boulders in the diamicton.

MNG16-C. Large sandstone clasts also exist within the diamicton ~150 km NNE of the proposed crater (Fig. 1*A*). One example shows the diamicton-tektite-silt series resting directly on sandstone bedrock (Fig. 5). In situ tektites near this exposure reside within the normally graded diamicton at the same level as a cluster of angular cobbles of sandstone, about 20 cm below the diamicton-silt contact. The arrangement of this cluster and some others in nearby quarries suggests that clasts shattered upon impacting the surface of the diamicton.

Many pebbles within the upper half of the diamicton here are also sandstone and rounded quartz. But most of the pebbles are laterite, presumably of basaltic protolith, consistent with the HFSE indication of a basalt-like affinity for the matrix, even for that around the sandstone clasts (Fig. 5). This observation is remarkable given that the nearest basalt flows are on the northern flank of the Bolaven Plateau, 90 km to the southwest. By contrast, the silt bed does not exhibit a basalt-like affinity—its HFSE ratios mimic regional sandstone values. Whatever emplacement processes pertain for the upper diamicton here must include simultaneous deposition of the sandstone and basaltic debris and tektites. Similar concentrations of angular to subangular sandstone cobbles and boulders occur within the upper parts of the diamicton in other nearby exposures (*SI Appendix*, Fig. S13).

Fluvial clasts in the diamicton.

SNM23-D. In many outcrops near the Mekong and Sekong Rivers, the diamicton contains clasts akin to those in nearby fluvial deposits. Site SNM23-D is representative of a few hundred meters

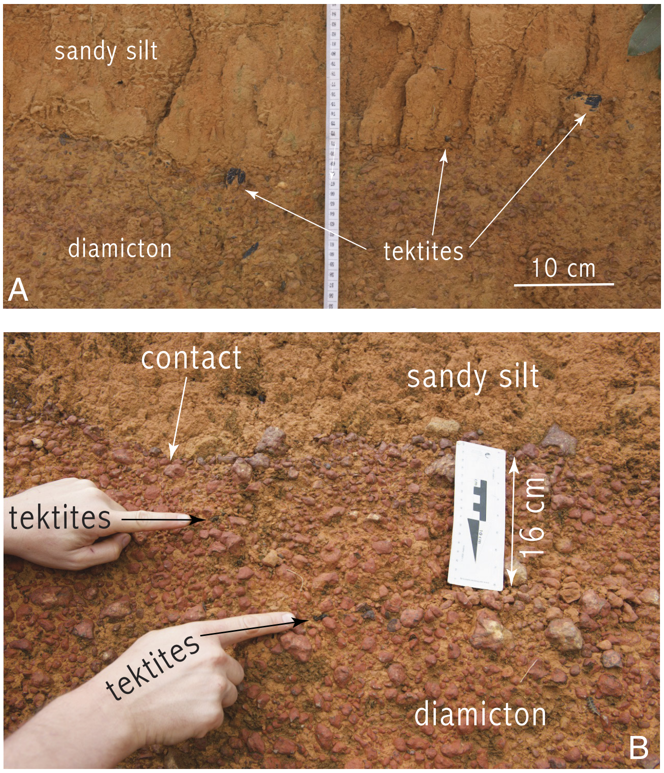

Fig. 3. Tektites at the diamicton-silt contact ~150 km NNW of the proposed impact site (*A*) (MNG16-F). Tektites within the upper 20 cm of the diamicton ~50 km SE of the proposed impact (*B*) (RDG15-C).

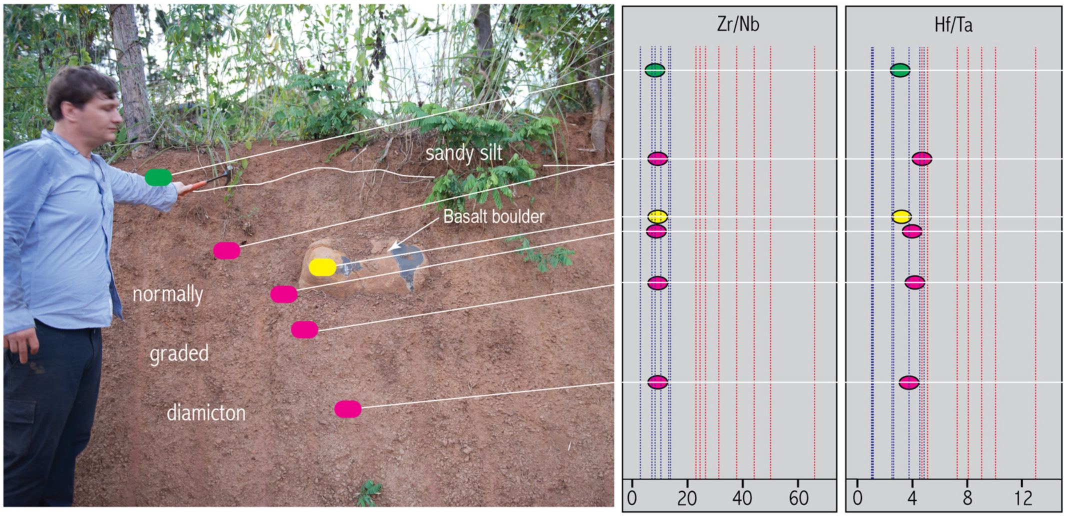

Fig. 4. Unweathered basalt boulder embedded in the upper part of the diamicton. Site NWF18-AD. The photograph shows silt, diamicton, basalt boulder, and sample locations. Charts show HFSE ratios for basalt boulder (yellow), fine matrix of diamicton (pink), and silt (green). Blue and red lines mark analyses of basalt boulders in lavas and sandstones on the Bolaven Plateau, respectively.

of adjacent quarry walls on the ancient Sekong River floodplain (*SI Appendix*, Fig. S14). Here, ~70 km southeast of the proposed impact, it lies directly upon a thick bed of vein-quartz-rich river gravel. Its contact with the silt bed is sharp but highly irregular, indicating either appreciable erosion of the top of the diamicton before deposition of the silt or a highly variable original thickness. Although angular pebbly laterite is abundant in the lower third to half of the diamicton, large, rounded pebbles and small cobbles of vein-quartz are also abundant. These clasts are indistinguishable in size, roundness, and composition from those of the underlying river gravel. This observation implies that clasts from the nearby floodplain were entrained during transport of the lateritic diamicton debris. In this exposure, the upper half to two-thirds of the diamicton consists of predominantly unrounded laterite pebbles. Less commonly and primarily on the plains of the Sekong River, the diamicton contains pebbles and cobbles of rounded vein quartz in its middle to upper portions (*SI Appendix*, Fig. S15).

Distal outcrops of the diamicton.

H1316-B. Two hundred km northwest of the proposed impact crater a thin layer of the pebbly diamicton lies on a broad plain, ~25 km northeast of and 50 m above the Mekong River. The presence of an overlying silt bed in sharp contact with this bed and a tektite 5 cm below its upper contact implies that it is the diamicton (*SI Appendix*, Fig. S16). The diamicton rests on an 8-cm thick, massive, blocky silt/clay layer, which in turn overlies an unconsolidated, laminated mud. This laminated bed overlies poorly sorted fine sand that may be overbank fines of an ancient Mekong River. The thin overlying massive silt/clay layer just beneath the diamicton implies minor bioturbation of originally laminated sediment prior to deposition of the diamicton.

Unlike the exposures we have described above, pebbles in this diamicton comprise two types of angular to subrounded fine-grained sandstone and rounded quartz pebbles as well as laterite. HFSE analysis of the matrix of the silt, the diamicton and the laminated mud reveals that all have an affinity with regional sandstones, not basalt. The abundance of rounded quartz pebbles implies that fluvial clasts, likely not from the plateau, were also incorporated into the diamicton.

ATP23-A. About 110 km southeast of the proposed impact site is a long exposure of the diamicton (*SI Appendix*, Fig. S17). It varies

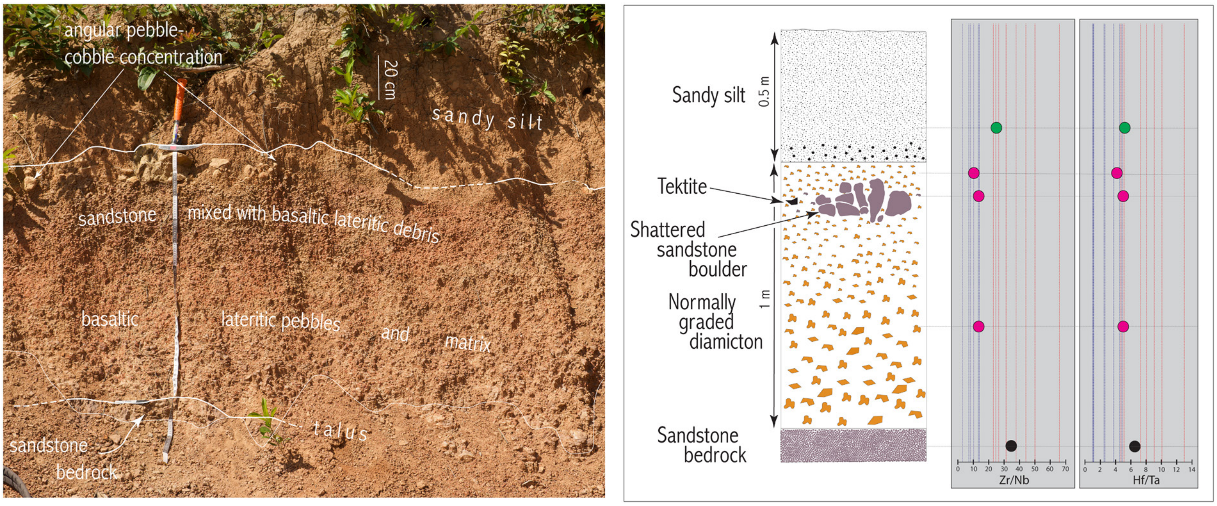

Fig. 5. Sandstone cobbles and boulders near the top of the diamicton ~150 km MME of the proposed crater. MNG16-C. The photograph shows cluster of sandstone cobbles near the top of the diamicton. Pen near base of cut marks sandstone bedrock/diamicton contact. HFSE ratios show that the sandy silt (green) has the signature of BVF sandstones, whereas the matrix of the diamicton (pink) has the signature of basalt.

in composition here and, as at other distal sites (e.g., *SI Appendix*, Fig. S18), is discontinuous. In places it consists mostly of laterite clasts like those described at sites nearer the plateau; elsewhere angular to rounded quartz pebbles and small, broken, hexagonal quartz crystals predominate. Within the reach that is quartz-rich, angular small pebbles predominate, but subrounded large pebbles and small cobbles are common. One such cobble sits embedded in the outcrop with its long axis upright and broken, like an opening lotus blossom. Perhaps its orientation indicates it was broken upon landing and then held in position within the now-eroded silt bed, although disturbance by bioturbation cannot be ruled out. Similarly, in one lateritic-breccia section, angular, weathered basalt pebbles and cobbles form an isolated ~30 cm patch. We infer that both the quartz cobble and basalt cluster fractured in situ upon emplacement, as Tada et al. (10) have demonstrated for a tektite cobble near Huai Om.

Proximal sites on the plateau.

BHS15-G. The diamicton reaches its maximum thickness and coarseness on the Bolaven Plateau. *SI Appendix*, Fig. S19 is a map that provides the context of the most proximal sites. In its center is a 6-by-3 km domain of southeast-sloping, 50 m-high ridges, surrounded by postimpact basalt flows. Streams between the ridges run on flat-lying cross-bedded Mesozoic fluvial sandstone. At Site BHS15-G and nearby, laterite cobbles and boulders and tektites litter the surface (*SI Appendix*, Fig. S20). The cryptocrystallinity of the laterite suggests a basaltic protolith. The average long dimension of the largest boulders lying on the surface is 63 cm. A hand-dug, meter-deep pit revealed that the loose surficial cobbles and boulders are part of a natural deposit of framework-supported, poorly sorted, angular, predominantly lateritic debris (Fig. 6*A*).

Shattered, jig-saw-puzzle packed, angular sandstone and mudstone boulders in an exposure near the bottom of a ridge about 2 km to the northwest, differ greatly in both composition and texture from the bouldery laterite deposits [(11), their *SI Appendix*, Fig. S13]. They argued that these sandstone and mudstone boulders ejected and landed at ~450 m/s, shattering upon emplacement. Roadcuts along the road leading up from this deposit to the ridge top expose mostly pebbly breccia, but also laminated, weathered mudstone boulders (*SI Appendix*, Fig. S21). The silty bed covers much of the crest of the ridge as well as the upper meter or so of the boulder breccia near the base of the ridge. These relationships imply that the ridges comprise 50 m thick fingers of coarse ejecta, with sandstone and mudstone boulders at the base and a thin discontinuous veneer of the silt.

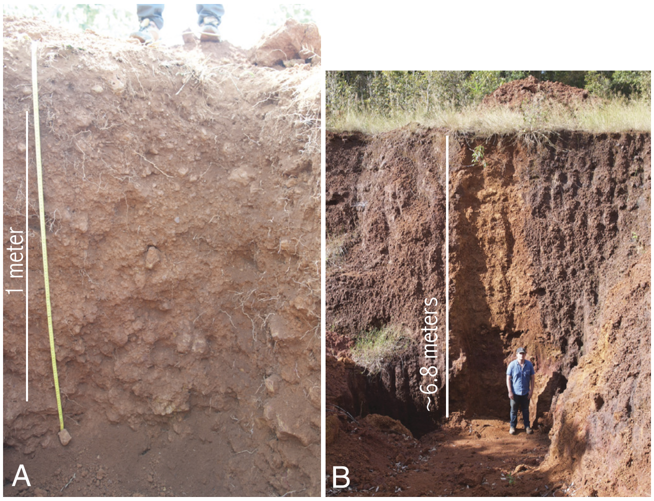

Fig. 6. Coarse lateritic diamicton deposits on the plateau SE of the proposed impact site. (*A*) Wall of hand-dug pit confirms the boulders extend too deeply to have been created by cultivation (BHS15-G). (*B*) An exploratory pit for laterite ~23 km SE of the proposed crater reveals very coarse upper 6.8 m of the breccia (LTE15-A).

LTE15-A. A 7-m deep exploratory pit, about 23 km southeast of the proposed impact site, made in search of economically viable laterite (14) reveals angular to subangular, commonly lumpy pebbles and cobbles of laterite (Fig. 6*B*). We saw no sandstone or mudstone fragments in our field inspection. Unaware of a possible impact origin of these deposits, (14) were puzzled that the trace-element chemistry of material in this and several other pits in the vicinity indicates a basaltic protolith, since the deposits lie upon sandstone bedrock. The base of the diamicton is unexposed in this pit, but a nearby site, SDD23-D, where the base is exposed, its thickness is 920 cm (*SI Appendix*, Fig. S22).

Isopach Map of Diamicton Thickness. The *SI Appendix*, Table S3 lists and Fig. 7 displays measured thicknesses of the diamicton. Two things are clear: First, large variations occur over short distances. Second, thickness increases toward and is greatest on the Bolaven Plateau.

Many long outcrops reveal that the thickness of the diamicton varies substantially over just a few tens to hundreds of meters. For example, in a large quarry a few km south of Pakse (*LST22-A*), thicknesses range from 240 to 490 cm over a distance only 160 m, and values ranging from 644 to 710 cm occur over just a few hundred meters in quarries 5 km farther west from the proposed impact site. Similarly, along a 90-m-long exposure at *H1319-A* (*SI Appendix*, Fig. S23), thicknesses vary from 14 to 22 cm. At the Chaiyaphum site (*SI Appendix*, Fig. S18), over 400 km west of the plateau, thicknesses range from zero to at least 60 cm over just a few tens of meters. Moreover, variations between sites a few km from each other show variations of tens of cm to >1 m.

Because these variations occur over distances shorter than the spacing of exposures, contouring is not justifiable. For example, between 60 and 180 km NW of the proposed crater, values vary from zero to 103 cm in no simply contourable way. At many locations, only a thin, discontinuous scattering of pebbles and tektites exist on near-horizontal bedrock surfaces. Sites like those may be what led some earlier workers (6) to conclude that the bed and its tektites are a lag deposit. However, these areas could also represent regions of thin deposition between thicker rays or patches [(15), p. 89)]. Likewise, short-distance variations on the plateau and its flanks defy attempts to contour thicknesses. For example, in the quarries immediately SE of Pakse, values range within just a few km from 240 to 714 cm. Many more exposures would be needed to confirm or dispute that spokes or rays, common features of lunar and planetary impact deposits, exist in this case.

Local variations notwithstanding, recorded thicknesses >300 cm are limited to <20 km outboard of the perimeter cliffs of the Bolaven Plateau and are more abundant on its western and southern flanks and on the southeastern part of the plateau. North and northwest of the plateau, thicknesses are predominantly <50 cm at distances >60 km. Closer, thicknesses are commonly >100 cm and are >300 cm at some sites (e.g., *SI Appendix*, Fig. S9). West and southwest of the plateau, values well under 100 cm occur at distances of ~60 to 100 km. In marked contrast, the large quarries and roadcuts 45 to 50 km west and southwest from the proposed impact site display thicknesses >200 cm and as high as 710 cm (for example, *SI Appendix*, Fig. S12). South of the plateau, excavations are commonly too shallow to expose the base of the deposit, but many show diamicton thicknesses to be >200 cm. One well-constrained measurement of 550 cm is 50 km south-southeast of the proposed impact site. At another site, ~35 km southeast of the proposed impact, the diamicton is 920 cm thick (*SI Appendix*, Fig. S22), and we have argued (11) that even more proximal to the impact (*SI Appendix*, Fig. S19) ridges

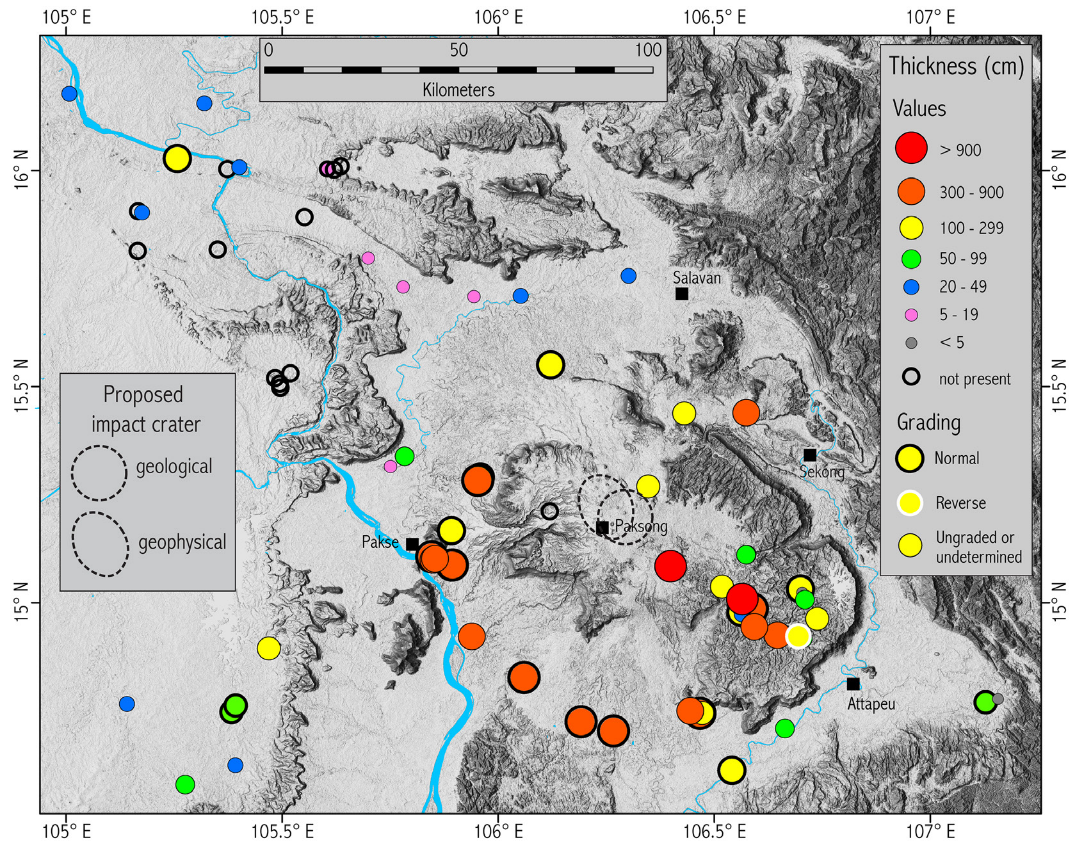

Fig. 7. Map of diamicton thickness shows increases toward the proposed impact site.

of diamicton are ~50 m thick. These measurements show that thicknesses are greatest on the Bolaven Plateau, encompassing the proposed impact site but seemingly centered about 20 km south of it.

We call this poorly sorted, gravelly bed the Bolaven diamicton, a name that concisely represents both its geographic origin and its basic characteristic, just as the "Australasian strewn field" describes succinctly two basic aspects of the tektites.

Averaged Maximum Clast Sizes. Fig. 8 and *SI Appendix*, Table S4 present the averaged grain sizes (as described in the *Methodology* section and illustrated in *SI Appendix*, Table S5) for the largest clasts in the Bolaven diamicton visible at each site. Where the deposit is normally graded, we measured the largest samples in the lowest exposed portion of the outcrop. We calculated the average of the long dimension of many (usually 10) of the largest clasts at a site. The average of several of the largest clasts offers a more representative value for each site than would the size of the single largest clast.

Throughout the region, values <50 mm are common. Only within ~70 km of the proposed impact crater do values exceed 50 mm. All but one of the sites with maximum clast averages >100 mm are near the center or the southeastern quadrant of the plateau. As with the thickness, local variations (for example, near Pakse and in the southeast quadrant of the plateau) argue against attempting a contour map.

The swath of large values south of the proposed impact site may be a genuine regional feature, but it may also reflect a geographic alias in our sites—we have few proximal sites north of the proposed impact site because of the extensive cover of postimpact basalt flows. If real, however, the southward skew in both the diamicton's clast-size and thickness patterns could mimic the marked asymmetry of the tektite strewnfield toward the southeast (e.g., ref. 16), which has been interpreted to indicate that the impactor approached from the Northwest.

The Tektites. Although our focus here is not the tektites, their close relationship to the Bolaven diamicton encourages a few observations relevant to understanding the manner and timing of their and the diamicton's deposition. During our field work, we collected in situ and locally ex situ tektites from nearly 250 sites. These were overwhelmingly of the Muong Nong (MN)-type and were all within 460 km of the proposed impact site (*SI Appendix*, Table S6). At all these sites, their total mass at any one site is far less than the total diamicton mass at that site, consistent with the calculation of ref. 5.

Fig. 9 shows the individual masses of our and previously published tektites *versus* distance from the proposed crater (*SI Appendix*, Fig. S24). By far, the largest tektites are MN-type, and they are the only type within 200 km of the proposed impact site. Within 130 km, the mass of the heaviest MN tektites at each site increases with distance. Beyond 160 km, maximum masses of MN tektites decrease with distance.

Within 100 km, the size of Bolaven diamicton clasts anticorrelates with the size trend of the tektites (compare Figs. 8 and 9). For example, at the site with the largest lateritic diamicton clasts (average max = 63 cm), the tektite masses are 0.5 to 1.5 g, whereas at the two sites of our most massive in situ tektites (184 and 486 g), average maximum dimensions of the diamicton clasts are 4.3 cm. This relationship is likely important for differentiating the processes that delivered the tektites and the diamicton.

The Silt Bed. We spent very little time investigating the silt bed that overlies the Bolaven diamicton, so our results are too incomplete to include in the main text. For future reference, though, what we have done appears in *SI Appendix*, Figs. S25–S29 and associated text. Here we make only a few general comments that will be useful in placing the silt into the context of impact processes.

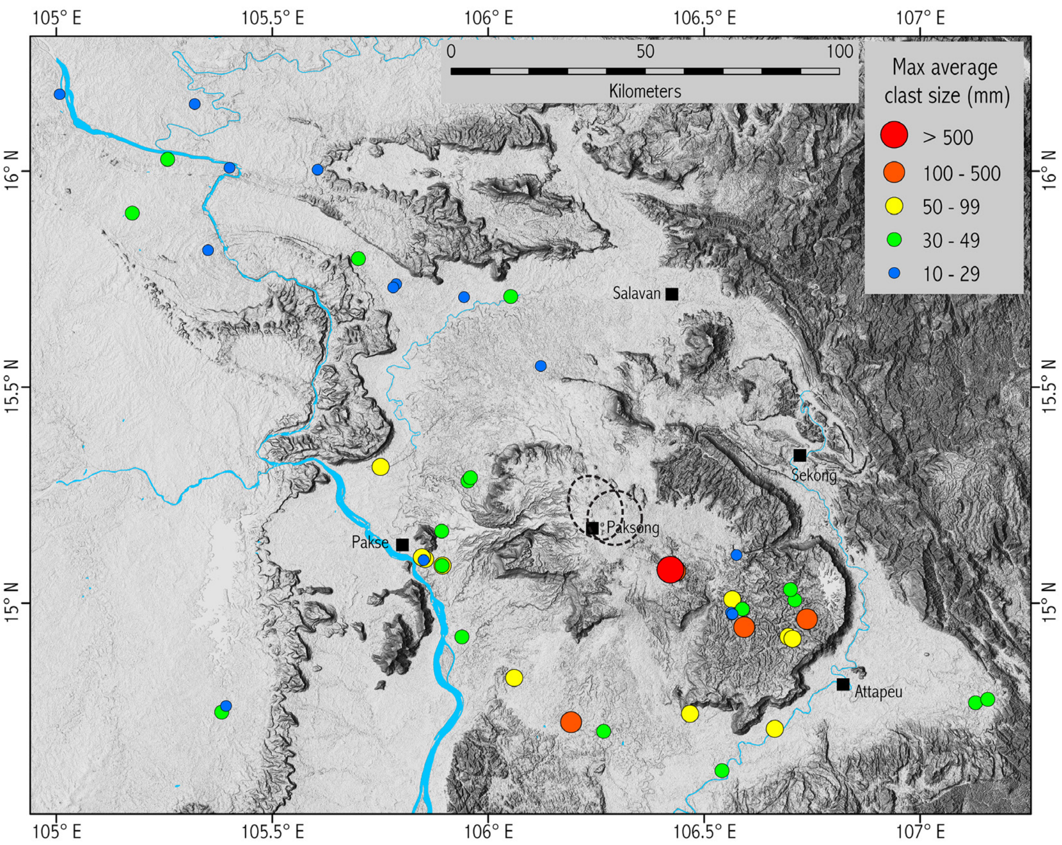

Fig. 8. The map shows that average diameters of the largest clasts are highest 20 to 60 km southeast of the proposed impact crater.

We have shown clearly that the silt bed overlies the diamicton in sharp contact throughout the region of our investigation. In many exposures, the bed is a meter or more thick, but absence of the bed and thicknesses of just a few tens of centimeters are common. We found no clear thickness pattern except that in the area of *SI Appendix*, Fig. S25 all observed thicknesses greater than about 200 cm lie south of the 200 cm contour.

In the few places where we have inspected it carefully, it is normally graded and massive (*SI Appendix*, Figs. S26–S28). Commonly, the basal portion of the silt is rich in angular granules (*SI Appendix*, Figs. S25, S26, and S29). Also, it is commonly disturbed in its upper portions, by both agriculture and natural erosion.

Finally, we observe that the composition and color of the silt bed varies markedly. Of the six sites where we analyzed the silt's HFSE ratios, two exhibit similar values to the basalts of the BVF and four have ratios similar to regional sandstones. The color of the silt ranges from pale tan to dark orange brown. Based on the HFSE findings, we tentatively interpret the tan colors to indicate a quartz dominance and the darker orange and brown colors to indicate a basaltic dominance.

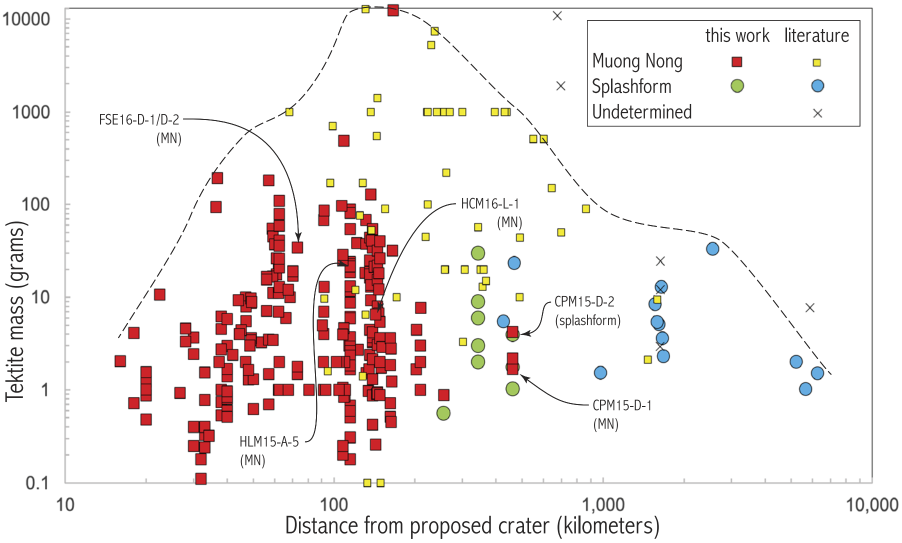

Fig. 9. In situ tektite mass vs. distance from the proposed impact. Only MN types occur within 200 km. They increase in maximum size out to 130 km and decrease from 160 km. The five named samples yielded ^{40}Ar-^{39}Ar dates for the impact.

Discussion

Increases in thickness and coarseness of the Bolaven diamicton toward the Bolaven Plateau (Figs. 7 and 8) imply that its source is on the plateau. The abundance of basaltic material reinforces this conclusion because both the BVF and the proposed crater are centered on the western part of the plateau (*SI Appendix*, Fig. S30). Furthermore, the undisturbed, sharp contact between the diamicton and overlying sandy silt with tektites in between implies that both date to the time of the impact.

Interpreting Bolaven diamicton stratigraphy requires at least a cursory understanding of hypervelocity-impact processes and deposits. Melosh's (15) explanations are particularly helpful in this regard, so we start with a primer of relevant information from that book. Fig. 10 shows five basic domains of target materials in a crater. The impactor and target materials closest to the impact site are vaporized and mushroom out of the crater at velocities approaching the incoming velocity of the impactor, that is, tens of km/s (15). Surrounding this region are melted materials that form a hemispheric shell, the ejected parts of which become tektites. Constructive interference of the initial compressional wave reflecting downward off the ground surface and the initial rarefaction wave produces spalled material, ejected as large blocks, also at velocities approaching that of the impactor, before the rest of the crater begins to excavate. Materials in the lower part of the crater are displaced downward and outward but are not ejected. On the flanks of the melted hemisphere is a quasi-torus of nonmolten material that is ejected from the crater.

Fig. 11 illustrates important details about the ejected materials. The unmelted materials that are to be displaced and ejected are fractured in tension within a few seconds of impact by the rarefaction wave, which travels at the speed of sound in rock (a few km/s). Those materials nearer the impact site experience higher stresses and thus a higher degree of comminution than materials closer to the eventual perimeter of the crater, which experience lesser stresses and thus are fractured less. So clasts farther from the impact site appear progressively larger and cooler in the figure.

Clasts in the displaced and ejected regions travel along curved streamlines within conceptually confined corridors referred to as streamtubes, at velocities that are high but significantly lower than the impactor's incoming velocity. The concept of streamtubes is useful to indicate that all particles along a streamline move roughly along the same path through the excavating crater. Excavation occurs sequentially outward and downward and at progressively lower velocities. Clasts moving along the shorter and higher route 1 exit the crater sooner and faster than material in longer and deeper routes 2 to 6, which exit progressively later and more slowly.

Once a particle reaches the ground surface, it launches into a ballistic trajectory through the atmosphere (Fig. 12). Clasts launched nearer the impact site have higher, faster, and longer trajectories (Trajectory 1), but because they originate from subterranean paths that are shorter, these trajectories contain less debris. Debris that launches nearer the perimeter of the crater is more abundant because it emerges from longer underground paths, has lower launch velocities, and follows shorter, lower trajectories (Trajectory 6). Large clasts follow ballistic trajectories and land at their launch velocity. In Earth's atmosphere, though, finer particles deviate from ballistic paths as they are subjected to atmospheric interference.

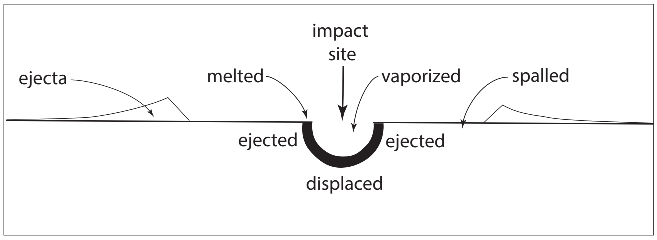

Fig. 10. Target material in a high-velocity-impact crater has five distinct domains—vaporized, melted, spalled, displaced, and ejected. Adapted from figure 5.13 of ref. 15.

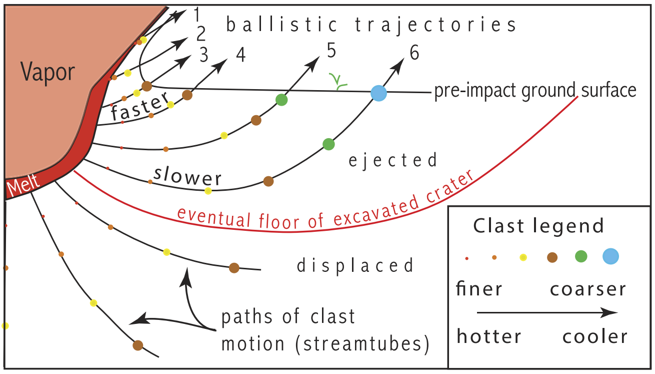

Fig. 11. Particles within the developing crater are progressively excavated along underground paths that arc outward from the impact. Melt lining the impact cavity is the last to exit along the arcs, in close pursuit of the finest unmelted material in the excavating crater. Adapted from figure 5.9 of ref. 15.

Together, the launched debris forms an "ejecta curtain," an expanding, open-upward cone of debris that comes to rest on the surrounding landscape. The four sloping dashed lines show the position of the ejecta curtain at times T through 2.5T. The figure shows the debris in transit at time T and at the four times when all debris from Trajectories 3 through 6 have landed. Particles higher in the ejecta curtain comprise less total mass, are smaller, travel faster and farther but land later than those lower in the curtain. Thus, one would expect the blanket of debris from the ejecta curtain to fine and thin and land later and at higher velocities with distance. Material in the melt hemisphere would be the tektite cabooses of each underground train, the last to launch from it and the last to land.

Origin of the Bolaven Diamicton and the Tektites. Melosh's (15) model predicts the diamicton's prevalent normal grading and the position of the tektites at or near its top. The presence of sandy, silty matrix throughout the typical outcrop could be a consequence

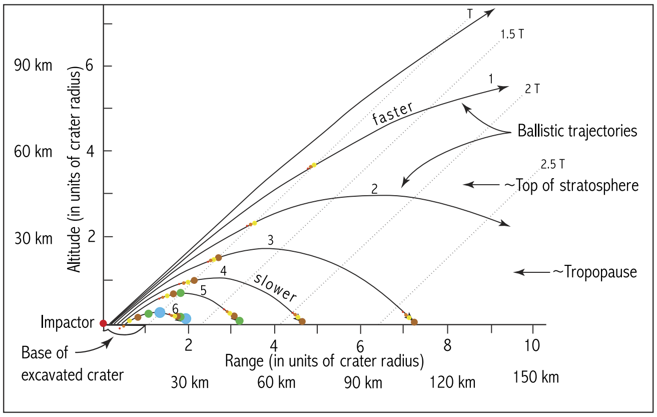

Fig. 12. Deposition from the ejecta curtain forms normally graded deposits that fine and thin with distance. The velocity of landing clasts increases with distance from the impact. Adapted from figure 6.4 of ref. 15, with speculative estimates of altitude, tropopause, and stratosphere added.

of fracturing as materials moved along their underground paths and could also reflect the similarly fine-grained saprolitic portions of the BVF target.

The model also predicts the geographic variation in MN-type tektite masses. The masses of the largest MN tektites increase with distance from about a gram at ~20 km to several kg by ~100 km. Fracture during transit through the excavating crater could account for this observation, providing the tektites were no longer ductile while traveling underground. MN tektites travelling longer underground paths would experience longer paths before launch and, hence, be subject to more collisions and greater comminution than tektites traveling shorter underground paths. Thus, one might expect tektites travelling route 1 to have suffered less fracture and thus be larger than those travelling route 6.

At distances beyond ~200 km, outboard of the peak of MN-tektite mass, the tektites are a nearly equal mix of MN- and aerodynamically shaped “splashform” types. Splashform shapes indicate launch while still molten and malleable and avoidance of brittle fracture. We posit that these exited the impact site at such high launch angles that they did not travel underground routes. Instead, they were launched directly into the atmosphere from nearer the inner surface of the melt hemisphere. That launch position would be consistent with their having experienced higher melt temperatures, as evidenced by greater depletion of volatile elements (17) and higher launch velocities than the MN tektites, as shown by their wider geographic distribution. The increase with distance in tektite ^{10}Be content (18, 19) also suggests that the melt hemisphere was stratified, with material from the surface of the target forming the innermost hemisphere and being the most far-flung.

Spalling and Disturbance by the Shock Waves, before Arrival of the Ejecta Curtain. At several localities near the edge of the impact crater, very large, angular quartz-rich sandstone boulders lie on but detached from underlying sandstone bedrock (*SI Appendix*, Figs. S2*D* and S7, and figure S16 of ref. 11). These commonly several-meter-wide boulders are usually tilted, but are not overturned, so they cannot be spall plates thrown far from the impact site. Their size and lack of internal weathering suggest they cannot be due to weathering or bioturbation. We speculate that they are plates broken loose while spallation was occurring but at or near the distal edge of the spall region, where shockwave stresses were high enough to detach them from the underlying bedrock but not to launch them more than a meter or two above their original position. The same process may explain jumbles of smaller angular sandstone and laterite boulders tens of km farther from the impact site (*SI Appendix*, Fig. S2 *A*–*C*), although dislodgement by the roots of large trees toppled by the force of either the shock wave or the ejecta curtain also seems plausible for these.

Erosion of substrates by the ejecta curtain. Incorporation of local materials into the deposits of the ejecta curtain is an expected consequence of the high horizontal velocity of ejecta-curtain debris [Melosh (15), his figure 6.4 and related text]. Especially at increasing distance from an impact site, velocities are high enough to entrain local debris via reptation (dislodging of substrate by the impact of clasts within the ejecta curtain) or differential air pressures great enough to cause fluidization (20). This scenario appears to be the case at many sites around the Bolaven Plateau (for example, PKQ22-C, HKG15-B, and SNM23-D). However, reptation and fluidization were not the only mechanism that incorporated local debris into the diamicton. At Site ATP23-A tektites lie among shattered angular vein-quartz pebbles, cobbles, and crystals, locally without the usual lateritic debris (*SI Appendix*, Fig. S17). We speculate that these thin sprays of quartz and tektites are the result of strong winds that swept out from the impact site or fluidization that dislodged local clasts beyond the reach of the ejecta curtain. Fluidization of debris must also have occurred during deposition of the diamicton, given the channel-filling geometry at some sites (*SI Appendix*, Fig. S18).

Basalt and Sandstone Boulders in the Upper Parts of the Diamicton. Basalt boulders in the upper parts of the Bolaven diamicton occur only within about 60 km of the impact site, always either upon or near in situ basaltic lavas (*SI Appendix*, Fig. S7). The simplest explanation is that the boulders were picked up from nearby basalt flows. However, it is hard to imagine how these large clasts could have been picked up after the bulk of the ejecta curtain had already thickly mantled the nearby lava flows. Moreover, there are hints that the boulders flew in from above (*SI Appendix*, Fig. S10) rather than floating on the top of a diamicton debris flow. We speculate that these boulders represent spalled materials that were launched into very high-angle ballistic trajectories. Even though they would have been launched at very high velocities and before development of the ejecta curtain, their trajectories could have been so high and long that they landed as deposition of the diamicton was complete or nearly so.

The large sandstone boulders found at and near the top of the Bolaven diamicton ~150 km north of the impact site may have a similar origin. They too show evidence of having broken apart upon impact at or near the end of diamicton deposition. At some sites, the sandstone boulders lie at the same level as MN tektites. This observation implies only that they landed at the same time, not that they took the same ballistic path.

Fig. 13 summarizes our suggestions for the regions within the crater from which the tektites, the diamicton and the spalled blocks came. All tektites originated within the melt hemisphere, but only the MN-type exited via underground paths. The more distal and higher-^{10}Be tektites originated closer to the inner edge of the melt hemisphere. The basalt and sandstone boulders near and at the top of the diamicton came to rest after ejection at high angles from the spalled region. Their higher and longer trajectories led to their emplacement after most of the diamicton. Blocks that lie below and at the base of the diamicton were either spalled at lower trajectories and landed before passage of the ejecta curtain or were created during passage of the initial shockwave, before arrival of the ejecta curtain.

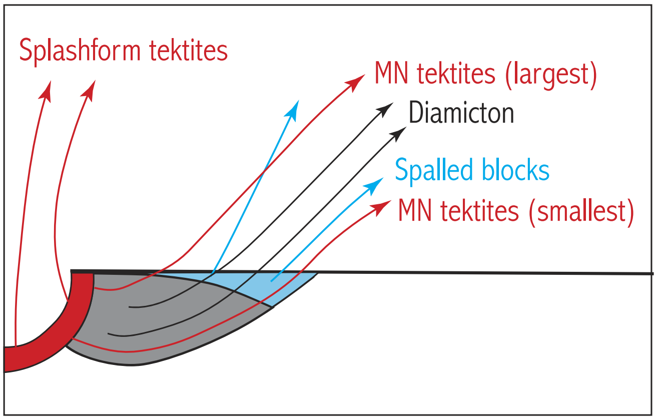

Fig. 13. Proposed source domains for the tektites and various diamicton components. Spalled blocks fly out at very high velocities before excavation of the crater. Splashform tektites come from the inner portions of the melt hemisphere and do not travel through the excavating crater. Diamicton clasts follow streamlines through the excavating parts of the crater, with MN tektites being the last to exit along each route.

Local Prevalence of a Basaltic Component in the Diamicton. At most sites we have visited, especially the ones proximal to the proposed impact site, the Bolaven diamicton appears to be predominantly laterized and saprolitized basaltic material, as evidenced in the *Results* section and *SI Appendix*. In contrast, at some more distal sites fine-grained sandstone clasts and matrix dominate. For example, at Huai Om, about 130 km from the proposed impact site and within the region of the largest tektites, the pebbles are predominantly quartz (9). Tektites from or beyond this distance from the impact crater also have a predominant quartz-rich sandstone component (e.g., ref. 1). Similarly, at the site displayed in *SI Appendix*, Fig. S23, both the framework and matrix are predominantly quartz sandstone.

Taken together, this referenced prior work and the observations we present are not compelling. However, we can speculate that the target rocks ejected shorter distances via the longest, deepest arcs through the excavating crater were predominantly basaltic and those thrown longer distances via the shortest, shallowest underground routes were predominantly sandstone. This proposal seems counterintuitive, given that the basaltic volcanic pile lies atop the sandstone. An alternative explanation might be that horizontal winds scouring the distal sites incorporated predominantly local, quartz-rich materials.

If the longer, deeper arcs delivered predominantly basaltic materials, then these deeper arcs must have excavated much from depths of less than a couple hundred meters because the thickness of the BVF is no greater than this (*SI Appendix*, Fig. S30). However, if the percentage of basaltic protolith in the tektites is commonly only 30 to 40%, as (11)'s Principal Component Analysis indicates, then the melt from which the tektites formed must have included much bedrock from greater depths as well.

A tentative solution may lie in a combination of the nature of ejection of the tektites and diamicton and the cross-sectional shape of the crater. If all splashform tektites and a large percentage of the larger MN tektites were ejected at high angles directly into the atmosphere from near the inner edge of the melt hemisphere, then sandstone protolith at the actual impact site could have been prevalent over basalt. Moreover, if the shape of the crater was not parabolic, but rather more like an inverted Mexican sombrero, because the far weaker saprolite and laterite of the basaltic pile was more easily shattered and excavated than the underlying bedrock (15), then basaltic protolith could have been prevalent in the ejected quasi-torus.

Conclusions

In the region of the Australasian strewnfield that contains tektites of predominately MN type, the tektites lie atop or within the upper parts of a diamicton of unmelted ejecta. The thickening and coarsening toward the Bolaven Plateau of this regionally extensive bed points to a source atop the plateau. The intimate association of this Bolaven diamicton with Australasian tektites supports the conclusion of ref. 11 that both were strewn from a crater buried by postimpact basaltic lavas of the BVF. We hope that these field observations and initial interpretations will provide starting blocks for future sedimentological analyses and physical modeling of the regional effects of this very large young extraterrestrial impact.

Data, Materials, and Software Availability. All study data are included in the article and *SI Appendix*.

ACKNOWLEDGMENTS. We are indebted to many who helped in the conduct of this work. These include our Lao drivers (Long and Phanthakone Syvilay), Singaporean undergraduate student Oh Jee Hon and Thai geologist Tawachai Chualaowanich for geological assistance in the field, Brian Wathen for preparing ^{40}Ar-^{39}Ar samples, the Chanthanalay family for their hospitality and occasional transport, and Nanyang Technological University professor Adam Switzer for supervising N.W. in his undergraduate granulometric analysis of the silt bed. The first few years of this work were supported by grants from the Earth Observatory of Singapore, which received most of its funding from the National Research Foundation Singapore and the Singapore Ministry of Education under the Research Centres of Excellence initiative. The final years of work were supported by the Taiwan Academia Sinica's Institute of Earth Sciences and private funds.

Author affiliations: [a]Earth Observatory of Singapore, Nanyang Technological University, Singapore 639798, Singapore; [b]Asian School of the Environment, College of Science, Nanyang Technological University, Singapore 639798, Singapore; [c]Department of Geosciences, National Taiwan University, Taipei 10619, Taiwan; [d]Institute of Earth Sciences, Academia Sinica, Taipei 11529, Taiwan; [e]Escuela de Geología, Universidad Industrial de Santander, Cra. 27 #9 Ciudad Universitaria, Bucaramanga CP 680002, Colombia; [f]Facility for Analysis Characterisation Testing Simulation, Nanyang Technological University, Singapore 639798, Singapore; [g]Department of Geoscience, University of Wisconsin-Madison, Madison, WI 53706; [h]Department of Geology and Mines, Ministry of Energy and Mines, Vientiane, Lao People's Democratic Republic; [i]Department of Mineral Resources, Ministry of Natural Resources and Environment, Bangkok 10400, Thailand; [j]Department of Earth and Planetary Sciences, Harvard University, Cambridge, MA 02138; and [k]Verisk, Extreme Event Solutions, Singapore 049481, Singapore

1. F. Jourdan, S. Nomade, M. T. D. Wingate, E. Eroglu, A. Deino, Ultraprecise age and formation temperature of the Australasian tektites constrained by ^{40}Ar/^{39}Ar analyses. *Meteorit. Planet. Sci.* **54**, 2573–2591 (2019).
2. E. P. Izokh, L. D. An, The geological position of the tektites and their significance for the Quaternary geology and geomorphology of VietNam. *Aktualni Voprosi Meteoritiki v Sibiri*, 206–231 (1988).
3. E. P. Izokh, L. D. An, Tektites of Vietnam: Tektites delivered by a comet–A hypothesis. *Meteoritika* **42**, 158–169 (1983).
4. J. T. Wasson, K. Pitakpaivan, P. Putthapiban, S. Salyapongse, B. Thapthimthong, Field recovery of layered tektites in northeast Thailand. *J. Geophys. Res.* **100**, 14,383–14,389 (1995).
5. P. S. Fiske, P. Putthapiban, J. T. Wasson, Excavation and analysis of layered tektites from northeast Thailand: Results of 1994 field expedition. *Meteorit. Planet. Sci.* **31**, 36–41 (1996).
6. P. S. Fiske *et al.*, "Layered tektites of Southeast Asia: Results of 1998 expedition to Laos and Vietnam" in *30th Annual Lunar and Planetary Science Conference* (Meteoritical Society, USA, 1999), pp. 157–761.
7. S. Bunopas *et al.*, "Australasian cometary impact, 0.8MA catastroloess buried alive Miocene, Pliocene Faunas in Thailand and central Australia, and Tektite-bearing flood deposits in NE. Thailand (Indochina), and australia impact fields" in *International Conference on the Geology of Thailand: Towards Sustainable Development and Sufficiency Economy* (Bangkok, 2007).
8. W. Songtham, D. C. Mildenhall, P. Jintasakul, J. Duangkrayom, "Evidence of sedimentary deposits generated by an Early Pleistocene meteor impact in northeastern Thailand" in *International Conference on Geology, Geotechnology and Mineral Resources of Indochina (GEOINDO 2011)* (Khon Kaen, Thailand, 2011), pp. 66–71.
9. T. Tada *et al.*, Identification of the ejecta deposit formed by the Australasian Tektite event at Huai Om, northeastern Thailand. *Meteorit. Planet. Sci.* **57**, 1879–1901 (2022).
10. T. Tada *et al.*, In situ occurrence of Muong Nong-type Australasian tektite fragments from the Quaternary deposits near Huai Om, northeastern Thailand. *Prog. Earth Planet. Sci.* **7**, 66 (2020).
11. K. Sieh *et al.*, Australasian impact crater buried under the Bolaven volcanic field, Southern Laos. *Proc. Natl. Acad. Sci. U.S.A.* **117**, 1346–1353 (2020).
12. J. Mizera, Quest for the Australasian impact crater: Failings of the candidate location at the Bolaven Plateau, Southern Laos. *Meteorit. Planet. Sci.* **57**, 1973–1986 (2022).
13. Japan International Cooperation Agency, Geological and mineral resources map of Lao People's Democratic Republic (Vientiane, Laos, 2008).
14. Y. Long, X. Yang, M. Yang, D. Zhang, Exploration and sources of bauxite deposit in the Bolaven plateau, Southern Laos. *J. Earth Sci.* **30**, 121–130 (2019).
15. H. J. Melosh, *Impact Cratering: A Geologic Process* (Oxford University Press, 1989).
16. B. P. Glass, Australasian microtektites and associated impact ejecta in the South China Sea and the Middle Pleistocene supereruption of Toba. *Meteorit. Planet. Sci.* **41**, 305–326 (2006).
17. C. Koeberl, Geochemistry and origin of Muong Nong-type tektites. *Geochim. Cosmochim. Acta* **56**, 1033–1064 (1992).
18. P. Ma *et al.*, Beryllium-10 in Australasian tektites: Constraints on the location of the source crater. *Geochim. Cosmochim. Acta* **68**, 3883–3896 (2004).
19. P. Rochette *et al.*, 10Be in Australasian microtektites compared to tektites: Size and geographic controls. *Geology* **46**, 803–806 (2018).
20. M. Rosenblatt, P. J. Hassig, D. L. Orphal, "Soil-air interactions during airblast-induced ground motions" (Report number DNA-TR-81-103, California Research & Technology Inc., Chatsworth, CA, 1982).